Towards a Plug&Play Solution for Real-Time Precise Positioning on Mass-Market Devices

Conference Paper · October 2020

DOI: 10.33012/2020.17623

CITATIONS
0

READS
47

2 authors:

Marco Fortunato
Sapienza University of Rome
10 PUBLICATIONS **38** CITATIONS
SEE PROFILE

Augusto Mazzoni
Sapienza University of Rome
67 PUBLICATIONS **721** CITATIONS
SEE PROFILE

Towards a Plug&Play Solution for Real-Time Precise Positioning on Mass-Market Devices

Marco Fortunato, DICEA, *Sapienza University of Rome*
Augusto Mazzoni, DICEA, *Sapienza University of Rome*

BIOGRAPHY

Marco Fortunato is a PhD candidate working on GNSS positioning and navigation. His research interests include the improvement of real-time GNSS navigation accuracy using mass-market devices with consolidated or innovative algorithms. He also collaborates with GMV NSL as a Research Engineer.

Augusto Mazzoni is an associate professor. His recent investigation topics are: Exploitation of Android GNSS raw measurements, GNSS based PVT estimation, high-rate GNSS for seismology, ground and infrastructures deformations control.

ABSTRACT

Despite pedestrian and vehicle navigation are the key applications enabled by the development of GNSS technology, the best approach to obtain accurate, reliable, continuous and robust PVT (Position-Velocity-Timing) solutions for this purpose has yet to be identified. The real limiting factor is the environment in which the users usually navigate: e.g. multipath effects and cycle slips in harsh urban environments strongly affect, respectively, pseudorange measurements and the continuity of carrier-phase observations. Therefore, positioning services relying on code-based algorithms cannot always meet the required accuracy – which varies depending on the targeted use case –; on the other hand, phase-based approaches as Real-Time Kinematic (RTK) and Precise Point Positioning (PPP) require strong effort to deal with the ambiguity term and its reinitialization when cycle slips occur. These problems are amplified when GNSS measurements from Android smartphone are considered due to the low-cost, linearly polarized and multi-purpose antenna which inevitably impacts on the quality of GNSS observables. This paper focuses on the performance analysis of GNSS POWER - an algorithm based on the loosely coupling between Single Point Positioning (SPP) solutions and variometric velocity - combined with IGS SSR corrections to increase the accuracy achievable in a real-time stand-alone solution. The integration of SSR corrections within GNSS POWER algorithm is validated in both static and kinematic scenarios using high-end GNSS receivers and Andorid smartphones. The results demonstrated the advantages of using SSR corrections on SPP and GNSS POWER solutions also on Android devices opening to new applications of real-time stand-alone positioning approaches on mass-market devices.

I. INTRODUCTION

Considering the latest developments in both space and ground segments, GNSS technology has nowadays become pervasive in civilian applications. In particular, the deployment of new constellations - e.g. Galileo, BeiDou and QZSS - , interoperable with GPS and transmitting signals on different L-band frequencies, enables more robust Position-Velocity-Timing (PVT) solutions. For instance, the availability of GNSS measurements on L5-band, leveraging a wider bandwidth and an improved signal structure with respect to L1, increases the resistance to multipath and other environmental effects [1, 2]. The development of new GNSS-based applications and solutions is also fed from new multi-frequency and multi-GNSS low-cost and mass-market receivers as the U-blox ZED F9P or the Broadcom BCM47755. The latter, in particular, brought multi-frequency GPS and Galileo L1/E1 and L5/E5a in Android smartphones revolutionizing the hierarchy within the mass-market world and electing Android devices as new leading products in this sector. However, a still open problem in GNSS-based kinematic processing is the identification of the best approach to provide continuity, reliability and high-accuracy in PVT solutions also in harsh environments. In fact, when the main requirement is high-accuracy, phase-based positioning algorithms - e.g. Real-Time Kinematic (RTK) [3], Precise Point Positioning (PPP) [4] or PPP-RTK [5, 6] - are considered. Accuracy at level of few centimetres or decimetres is although achievable only with successful ambiguity handling consisting in both detecting cycle slips and fixing, when possible, carrier-phase ambiguities [7, 8]. Urban environments, on the other hand, are notoriously challenging for phase-based positioning techniques due to the low tracebility and continuity of phase measurements which impacts also on the convergence of the associated estimation algorithm [9, 10]. Kinematic applications not requiring accuracy at centimetres level but claiming for continuous solutions can rely on code-based positioning techniques, as Single Point Positioning (SPP). However, due to multipath effects on pseudorange measurements, the accuracy can be degraded up to tens of metres [11]. In this case, detecting and down-weighting or removing faulty measurements is crucial to ensure reliable solutions.
Sapienza University of Rome is responsible for the development of GNSS POWER (POsitioning and Variometric Velocities Estimation in Real-time), a real-time processing tool based on a loosely coupling approach between an SPP solution and the

kin-VADASE (kinematic Variometric Approach for Displacement Analyses Stand-alone Engine) [12] velocities estimated from phase measurements, which enables accuracy of few decimetres and millimetres/second in the positioning and velocity domain respectively. GNSS POWER, not requiring any ambiguity fixing strategy or external corrections, allows to retrieve immediately accurate positions and velocity targeting applications where the key requirements are low convergence time and continuity. Although the lower performances in the positioning domain with respect RTK or PPP due to the use of a code-based solution to define the absolute user position, the achievable sub-meter accuracy opens to a wide range of kinematic applications as addressed in [13]. Similar solutions have been proposed from different researches to provide increased accuracy especially in the case of smartphone navigation [14, 15, 16]. The aim of this work is to exploit real-time State Space Representation (SSR) corrections available from the Real-Time Service (RTS) supported from International GNSS Service (IGS) to account for satellite orbit/clock corrections and code biases within GNSS POWER algorithm to improve the final positioning accuracy. In fact, despite the main use in real-time PPP solutions [17], SSR corrections can be useful also within code-based processings as demonstrated in [18].

This Introduction is followed by the description of GNSS POWER and SSR concepts and the final integrated solution (Section II.). Section III. shows the results obtained combining GNSS POWER processing and SSR corrections in both static and kinematic scenarios. The results are then discussed and summarized in Section IV..

II. METHODOLOGY

This section deals with the description of the positioning algorithm used within this work. The attention is also focused on SSR corrections and how they are integrated within GNSS POWER to increase the final PVT accuracy.

1. GNSS POWER

The Geodesy and Geomatics Division of Sapienza University of Rome is responsible for the development of GNSS POWER with the aim of providing real-time stand-alone high-accurate PVT solutions. The algorithm is based on a loosely coupling approach which combines the absolute receiver position, estimated using a SPP (Single Point Position) algorithm, and the velocity, obtained using the kin-VADASE (Variometric Approach Displacement Analysis Stand-alone Engine)[12]. GNSS POWER relies on both pseudorange and carrier-phase observations (Fig. 1). In particular, kin-VADASE estimates real-time 3D velocity with accuracy at level of few mm/s [19, 20] based on the variometric phase measurements, i.e. the time variation of carrier-phase observations. The use of differenced phase measurements allows to neglect, if no cycle slip occurred between two consecutive epochs, the phase ambiguity terms leading to instantaneous and reliable estimated velocity. Based on a WLS (Weighted Least Squares), no convergence time is required also from the SPP algorithm implemented within GNSS POWER. Therefore, GNSS POWER targets applications where reliability, continuity and very low convergence time are the main requirements. On the other hand, GNSS POWER, relying on code measurements for the absolute receiver position, is suitable for application with requirements up to different decimetres.

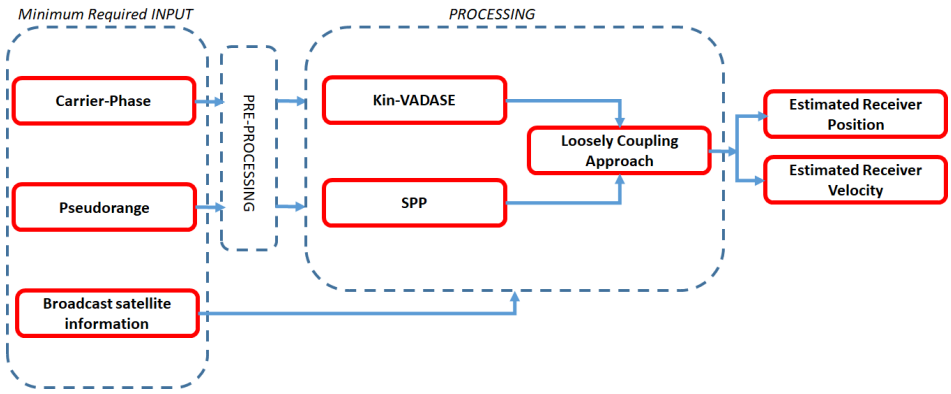

Figure 1: GNSS POWER high-level architecture

2. SSR corrections

The IGS, through its RTS program, is currently streaming SSR corrections following RTCM standard and NTRIP protocol to support real-time PPP applications. The real-time streams provided by the IGS, and computed from the different analysis centers, contain corrections to the broadcast satellite orbits and clock and satellite code/phase biases [21]. The following sub-sections deal with the SSR corrections used within GNSS POWER describing their mathematical model.

a) Orbit corrections

Precise orbits ($X_{precise}$), in ECEF (Earth Centered and Earth Fixed) reference frame, can be obtained combining the satellite broadcast coordinates ($X_{broadcast}$) and the SSR corrections (δX) as follow [21, 22]:

$$X_{precise} = X_{broadcast} - \delta X \tag{1}$$

However, it is worth to mention that SSR corrections are provided in the coordinate system of satellite orbit - i.e. hence radial, along-track and cross-track - and a coordinate transformation is required before they can be applied. In particular, δX can be expressed on the basis of the following equation:

$$\delta X = [e_{radial}\, e_{along}\, e_{cross}]\delta O \tag{2}$$

where: e_{radial}, e_{along} and e_{cross} are the three unit vector on radial, tangent and normal of satellite position. These can be computed based on satellite position (X_{sat}) and velocity (V_{sat}):

$$e_{along} = \frac{V_{sat}}{\mid V_{sat} \mid} \tag{3}$$

$$e_{cross} = \frac{X_{sat} \times V_{sat}}{\mid X_{sat} \times V_{sat} \mid} \tag{4}$$

$$e_{radial} = e_{along} \times e_{cross} \tag{5}$$

The complete orbit corrections vector (δO) is obtained in real-time, knowing the time difference between the current epoch (t) and the reference time specific for the SSR orbit corrections message (t_0), based on the transmitted parameters:

$$\delta O = \begin{bmatrix} \delta O_{radial} \\ \delta O_{along} \\ \delta O_{cross} \end{bmatrix} + \begin{bmatrix} \delta \dot{O}_{radial} \\ \delta \dot{O}_{along} \\ \delta \dot{O}_{cross} \end{bmatrix} (t - t_0) \tag{6}$$

b) Satellite clock corrections

In according to the literature [21, 23], SSR clock correction messages contain the 3 polynomial coefficients (C_0, C_1 and C_2) required to correct the broadcast satellite clock bias. In particular, the precise clock ($t_{precise}$), based on the broadcast satellite clock ($t_{broadcast}$) and the correction obtained from SSR messages (δt), follows:

$$t_{precise} = t_{broadcast} - \frac{\delta t}{Speed\, of\, light} \tag{7}$$

where δt can be derived knowing the current epoch (t) and the reference time epoch for the clock correction (t_0):

$$\delta t = C_0 + C_1(t - t_0) + C_2(t - t_0)^2 \tag{8}$$

c) Satellite code biases

The satellite code bias - caused by the satellite transmission circuit hardware design [18] - is commonly corrected in real-time applications using the broadcast TGD (Time Group Delay) or, if knwon, the DCB (Differential Code Biases) values. The SSR code biases correction messages contain signal dependent and absolute values that must be added to the pseudorange measurements of the corresponding code signal to obtain the corrected pseudorange value. In this case, TGD and/or DCB corrections must not be applied [21].

3. Integrating SSR corrections in GNSS POWER

In order to include SSR corrections, GNSS POWER architecture has been modified with an additional layer to handle SSR corrections (Fig. 2) in both real-time and post-processing scenarios. The additional layer consists of an RTCM decoder able to retrieve (from a binary file or a socket stream), decode and apply SSR orbits, clock and code biases corrections. Within GNSS POWER, SSR corrections are applied in the SPP algorithm in order to reduce the un-modelled errors due to satellite orbits

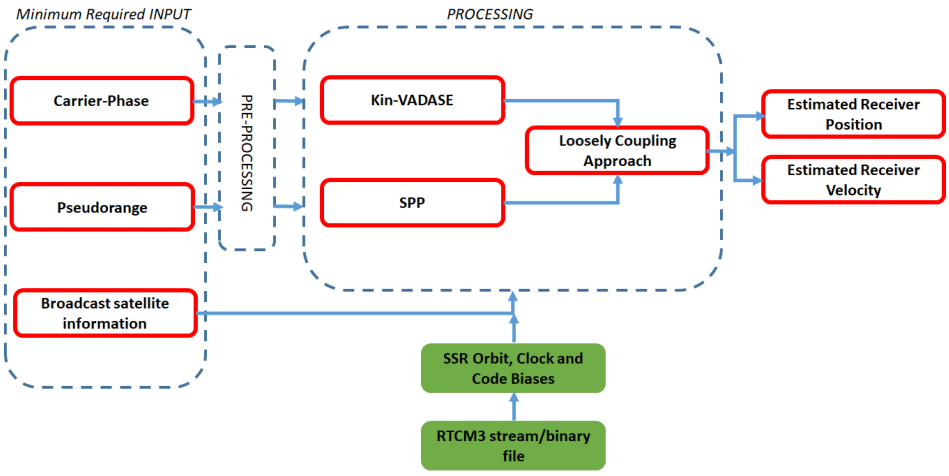

Figure 2: GNSS POWER high-level architecture including the SSR layer

and clock. In fact, the enhanced accuracy in orbits, below 10 cm, and clock, below 0.3 ns, parameters [23] allows to increase the positioning accuracy as well as the efficiency of pre-processing strategies to detect faulty measurements. Unfortunately, a still open problem for single frequency or uncombined multi-frequency users is represented by the residual ionospheric error. Currently, the lack of atmosphere corrections stream transmitted on a global scale through the IGS NTRIP caster leads to the use of Klobuchar [24] model in the above-mentioned cases. SSR corrections are not applied within the kin-VADASE algorithm due to their low impact on the processing of time-differenced carrier-phase measurements. In fact, the variation of SSR corrections between two consecutive epochs with high-frequency measurements (>1 Hz) can be considered negligible. This is also confirmed from the results obtained in previous researches including precise IGS products (orbits and clock) and variometric analysis [19]. Nevertheless, in Section III., the effects of orbits, clock and code biases corrections on the variometric phase measurements processing will be analysed.

III. VALIDATION

The effects of SSR corrections in GNSS POWER solutions are extensively evaluated in different test environments and conditions. The solutions illustrated in the following sections are obtained in real-time scenario. Based on the literature [23], CLK93 products, computed by CNES and redistributed through the IGS RTS (Real-Time Service), were collected in binary files for each dataset using the RTKLib 2.4.3 software library [25].

1. Static scenario

The performance achievable using GNSS POWER in combination with SSR corrections are firstly evaluated in static conditions using GNSS measurements from a permanent station: M0SE, one of the IGS/EUREF station placed in Rome (Fig. 3), was used in this test. The use of high-quality GNSS measurements in static conditions allows, in fact, to assess the methodology

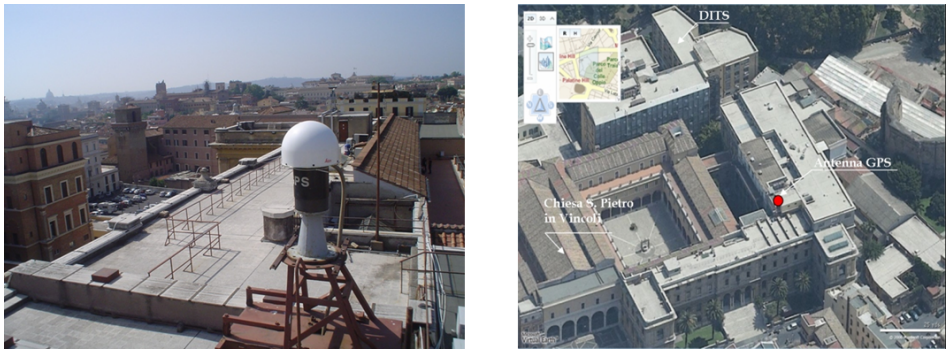

Figure 3: M0SE reference station and its location

and establish a benchmark, in terms of positioning accuracy, useful also to evaluate results coming from GNSS observations of poorer quality. The dataset was composed of 1 Hz GPS and Galileo observations collected in the period between the 25^{th} and the 31^{st} August 2020 - DOY (Day Of the Year) between 238 and 244. In order to facilitate the analyses, hourly processing sessions were performed and then combined in the daily solutions. This approach does not impact on SPP and kin-VADASE since they are based on simple WLS. The analyses were executed using GPS and Galileo L1/E1 observations with a cutoff angle of 10° to cope with poor quality measurements. The available precise IGS coordinates for M0SE station are used to evaluate the accuracy in this section.
In order to assess the contributions of SSR corrections on SPP, kin-VADASE and GNSS POWER, the results are here illustrated per algorithm.

a) SPP processing

The residual positions obtained using (BRDC + SSR) and not using (BRDC) SSR corrections for DOY 239 are shown in Fig. 4. The analysis of the residual positions demonstrates how the use of SSR corrections provides more stable, and reliable solutions in both horizontal and vertical directions. The statistical analyses, contained in Tab. 1, illustrates how analogous considerations can be extended to the other days in the dataset.

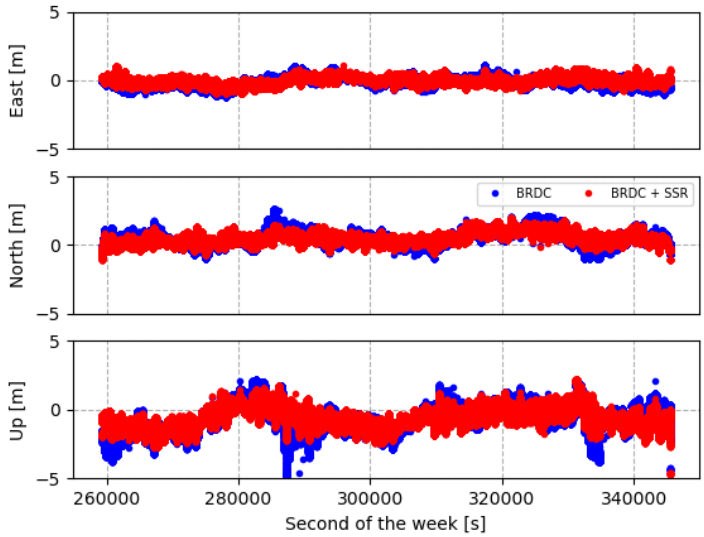

Figure 4: SPP residual position obtained, for the data acquired on DOY 239, with (red) and without (blue) SSR corrections

Table 1: Statistical analyses of SPP residuals with respect to the IGS precise coordinates in East, North and Up. The results are reported for both BRDC and BRDC + SSR processings

	BRDC						**BRDC + SSR**					
	East		**North**		**Up**		**East**		**North**		**Up**	
	Mean [m]	**Std. Dev. [m]**	**Mean [m]**	**Std. Dev. [m]**	**Mean [m]**	**Std. Dev. [m]**	**Mean [m]**	**Std. Dev. [m]**	**Mean [m]**	**Std. Dev. [m]**	**Mean [m]**	**Std. Dev. [m]**
238	-0.07	0.40	0.37	0.53	-0.52	1.23	0.04	0.31	0.35	0.36	-0.70	0.87
239	-0.10	0.35	0.56	0.56	-0.67	1.04	0.00	0.29	0.50	0.41	-0.60	0.75
240	-0.06	0.40	0.49	0.65	-0.36	1.35	-0.03	0.26	0.50	0.39	-0.51	0.73
241	-0.04	0.41	0.36	0.57	-0.48	1.23	0.00	0.29	0.38	0.34	-0.59	1.00
242	-0.28	0.38	0.43	0.56	-0.56	1.33	-0.21	0.28	0.51	0.40	-0.87	0.80
243	-0.09	0.38	0.48	0.80	-0.65	1.28	-0.01	0.32	0.55	0.45	-0.76	0.96
244	-0.07	0.32	0.50	0.64	-0.62	1.13	0.00	0.31	0.64	0.42	-0.73	0.75

Mean and standard deviations of Tab. 1 demonstrate marked improvements in both accuracy and precision when SSR corrections are applied. To facilitate the reader in the analyis of the results, an aggregated plot, representing daily mean and standard deviation in the form of error bars based on Tab. 1, is given in Fig. 5. The horizontal dashed lines represents the mean RMS (Root Mean Square) errors obtained on the weekly solutions. The error bars show immediately lower standard deviations and mean in the case of BRDC + SSR processing. The highest impact is observed for the Up component which is noisier and less accurate than East and North due to the use of Klobuchar [24] ionospheric model. The use of SSR corrections, reducing other unmodelled

errors - e.g. satellite orbits, clock and code biases -, improves also the accuracy in vertical direction. To sum up the statistical analysis, an improvement in the final RMS values of 22.7, 17.5, 20.0 % is observed in East, North and Up components: 0.39, 0.77 and 1.35 m are observed using only broadcast products, while 0.31, 0.63 and 1.08 m when SSR corrections are also applied in East, North and Up respectively.

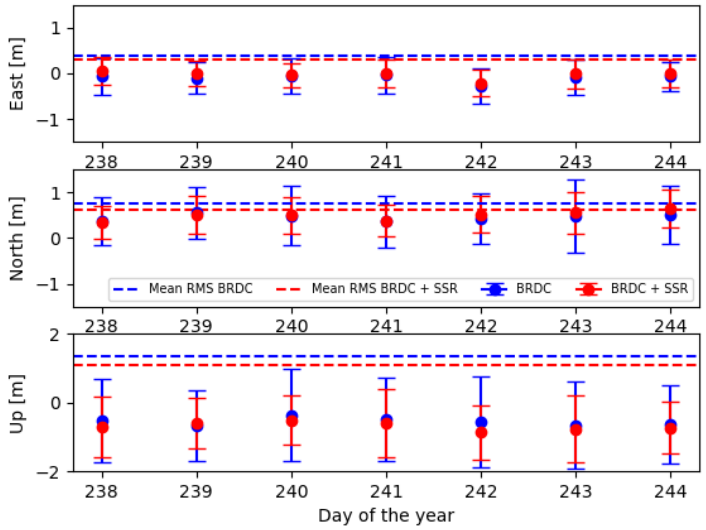

Figure 5: Aggregated statistical analyses of the SPP residuals obtained with (blue) and without (red) SSR corrections

b) kin-VADASE processing

The aim of this section is to investigate kin-VADASE performance in static conditions to demonstrate the negligible impact of ephemeris, clock and code biases corrections on the variometric velocity. The accuracy achievable using the variometric approach has extensively been tested in [19, 12, 26] demonstrating noise at level of few millimetres/second in both horizontal and vertical directions. For this reason, the analysis on this section will focus only on the data acquired on DOY 239. Tab. 2 highlights noise level of 1 mm/s for the horizontal components and lower than 3 mm/s in the vertical direction using only broadcast products. The use of SSR corrections increases the noise of variometric solutions mainly due to few outliers related to changes of SSR messages (Fig. 6): accuracy around 2 mm/s and 3 mm/s is observed in this case. The statistical analysis of difference between the velocity estimated with and without SSR corrections (Fig. 6) shows RMS of 1.4, 1.7 and 3.0 mm/s in East, North and Up respectively. These values are comparable with the noise level highlighted for kin-VADASE solutions demonstrating the low impact of SSR corrections in the variometric phase measurements analysis.

Table 2: Statistical analyses of variometric velocity residuals. The results are reported for both BRDC and BRDC + SSR processings

	East		**North**		**Up**	
	Mean [m/s]	**Std [m/s]**	**Mean [m/s]**	**Std [m/s]**	**Mean [m/s]**	**Std [m/s]**
BRDC	-2.34e-04	9.85e-04	-1.27e-05	1.27e-03	2.05e-05	2.58e-03
BRDC+SSR	-2.40e-04	1.77e-03	-1.63e-05	2.18e-03	1.16e-05	4.18e-03

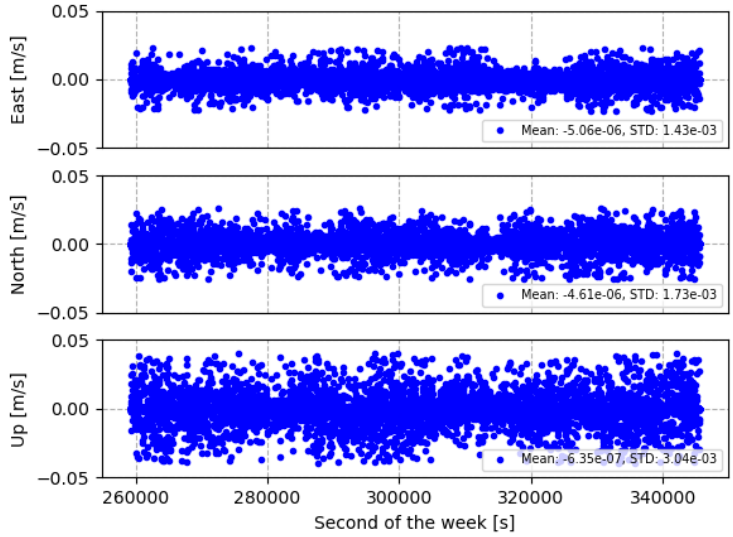

Figure 6: Differences between variometric velicity estimated with and without SSR corrections

c) GNSS POWER processing

SPP and kin-VADASE solutions represent the starting point for the loosely coupling approach leading to the final GNSS POWER PVT estimation. Dealing with results in the positioning domain, the structure of Section III.a) is here followed. Fig. 7 contains GNSS POWER residuals obtained in the case of broadcast only and broadcast ephemeris with SSR corrections for DOY 239. As highlighted in the case of Fig. 4, the use of SSR corrections improves the robustness of the estimation process: the residuals show lower dispersion and a reduced number of outliers. It is worth to mention that, due to the hourly processing sessions used in this analyses, GNSS POWER algorithm is re-initialised every hour using SPP solution increasing the expected standard deviation for the final PVT results. However, the statistical analysis of the residual GNSS POWER solutions (Tab. 3) shows an improvement in the final accuracy with respect the results obtained from SPP not only when SSR corrections are applied. The analysis of Tab. 3 shows a marked reduction and an increased stability of mean and standard deviation in the horizontal directions. Moving on to the Up component, if the use of SSR increases the precision by reducing the residual position standard deviations, the mean value increases, except for DOY 239. This is due to the initial position of GNSS POWER, based on the SPP results, which results, in the first epoch, less accurate for the days of analysis when SSR corrections are used. However, the aggregated results in Fig. 8 demonstrates an improvement in the RMS computed for the three components of 32.6, 18.2 and 18.2 % in East, North and Up. The difference between SPP and GNSS POWER performances, obtained using or not SSR corrections, are included in Tab 4 demonstrating all the benefits coming from the use of GNSS POWER and SSR corrections to improve the final PVT results.

Table 3: Statistical analyses of GNSS POWER residuals with respect to the IGS precise coordinates in East, North and Up. The results are reported for both BRDC and BRDC + SSR processings

	BRDC						**BRDC + SSR**					
	East		**North**		**Up**		**East**		**North**		**Up**	
	Mean [m]	**St. Dev. [m]**	**Mean [m]**	**St. Dev. [m]**	**Mean [m]**	**St. Dev. [m]**	**Mean [m]**	**St. Dev. [m]**	**Mean [m]**	**St. Dev. [m]**	**Mean [m]**	**St. Dev. [m]**
238	-0.165	0.354	0.369	0.477	-0.511	1.083	-0.012	0.257	0.347	0.287	-0.702	0.743
239	-0.175	0.289	0.566	0.514	-0.616	0.876	-0.046	0.231	0.503	0.349	-0.587	0.637
240	-0.13	0.369	0.529	0.561	-0.304	1.207	-0.074	0.202	0.506	0.33	-0.497	0.601
241	-0.129	0.375	0.362	0.502	-0.477	1.079	-0.048	0.241	0.39	0.269	-0.578	0.906
242	-0.362	0.331	0.448	0.51	-0.514	1.17	-0.26	0.235	0.524	0.336	-0.847	0.689
243	-0.217	0.335	0.526	0.746	-0.565	1.154	-0.081	0.258	0.57	0.395	-0.738	0.848
244	-0.175	0.269	0.481	0.629	-0.609	1.028	-0.051	0.258	0.641	0.388	-0.729	0.616

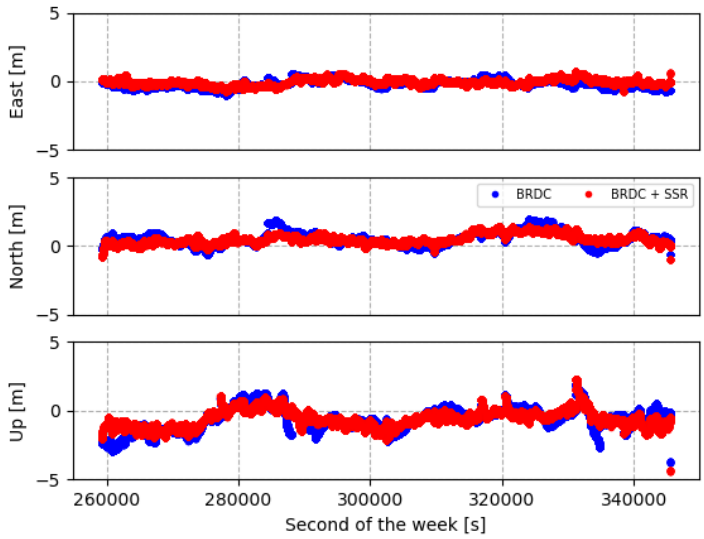

Figure 7: GNSS POWER residual position obtained, for the data acquired on DOY 239, with (red) and without (blue) SSR corrections

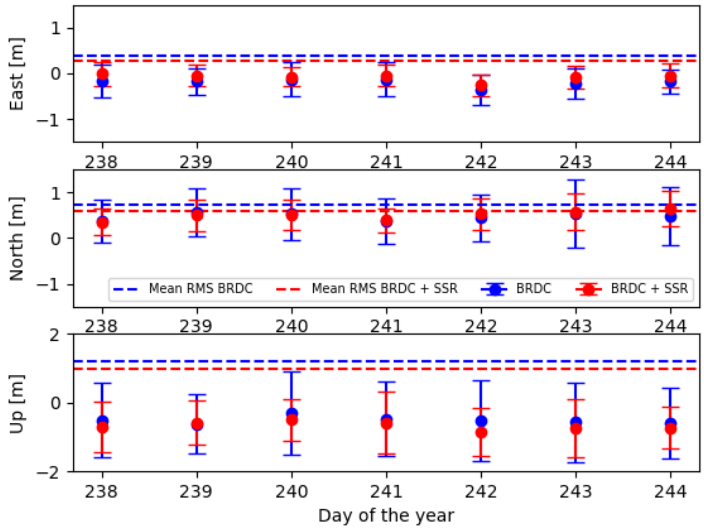

Figure 8: Aggregated statistical analyses of the GNSS POWER residuals obtained with (blue) and without (red) SSR corrections

2. Kinematic scenario

The results obtained in static scenario encouraged the collection of a dataset in kinematic conditions. On the 29^{th} August 2020, a car equipped with a geodetic receiver (GeoMax Zenith35 Pro), a Xiaomi Mi 8 and a Google Pixel 4 was used to drive, for a period of almost 25 minutes, within Rome. An open sky environment, with few trees and buildings on a limited portion of the selected path, was considered for this test. In particular, the same path was repeated 7 times in order to evaluate the repeatability of the final GNSS POWER solution (Fig. 9). The 3 GNSS devices were placed, aware of the non-optimal tracking conditions, inside the vehicle (Fig. 10) in order to collect GNSS measurements simulating the mean smartphone users behaviour. The acquisition rate was set to 5 Hz for the geodetic receiver, while the acquisition rate for the Xiaomi Mi 8 and the Google Pixel 4 is fixed to 1 Hz without the possibility to adapt it. Rinex ON app was used to collect measurements from the two smartphones. The reference track, necessary to evaluate the accuracy achievable using GNSS POWER and SSR corrections, was obtained

Table 4: RMS values obtained for SPP and GNSS POWER algorithms in East, North and Up. The results are reported for both BRDC and BRDC + SSR processings

	RMS [m]											
	BRDC						BRDC + SSR					
	SPP			GNSS POWER			SPP			GNSS POWER		
	East	North	Up	East	North	Up	East	North	Up	East	North	Up
238	0.40	0.64	1.34	0.39	0.60	1.20	0.31	0.50	1.12	0.26	0.45	1.02
239	0.36	0.79	1.24	0.34	0.77	1.07	0.29	0.65	0.96	0.24	0.61	0.87
240	0.40	0.82	1.40	0.39	0.77	1.25	0.27	0.63	0.89	0.22	0.60	0.78
241	0.41	0.67	1.32	0.40	0.62	1.18	0.29	0.51	1.16	0.25	0.47	1.07
242	0.47	0.70	1.45	0.49	0.68	1.28	0.35	0.65	1.18	0.35	0.62	1.09
243	0.39	0.93	1.43	0.40	0.91	1.29	0.32	0.71	1.22	0.27	0.69	1.12
244	0.32	0.81	1.29	0.32	0.79	1.20	0.31	0.77	1.04	0.26	0.75	0.96

through the analysis of the 5 Hz measurements collected with the geodetic receiver using the NrCan PPP online service [27].

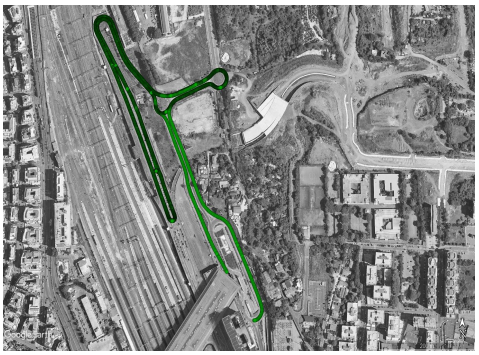

Figure 9: Path followed in kinematic scenario

Figure 10: GNSS receivers setup inside the vehicle

The attention is here focused on the accuracy achievable with SPP and GNSS POWER algorithms when SSR corrections are used (BRDC + SSR) or not (BRDC). In this case, SPP solutions were obtained using RTKLib 2.4.3 software package in order to have an independent solution with respect GNSS POWER architecture. GPS and Galileo L1/E1 measurements with a cutoff angle of 10° and C/N_0 threshold of 30 dBHz werre considered in the different processing. Fig. 11 illustrates the results obtained using the GeoMax Zenith35 Pro. Fig. 11a shows the residuals obtained, using the aforementioned processing strategies, in a local reference frame. Fig. 11b represents the CDF (Cumulative Distribution Function) obtained for the horizontal residuals for the 4 processing approaches investigated. The results for the Xiaomi Mi 8 and the Google Pixel 4 are shown in Fig. 12 and Fig. 13 respectively. The y-axis in Fig. 11a, Fig. 12a and Fig. 13a is limited between -10.0 and 10.0 m in order to highlight differences between the selected processing methodologies. The statistical analysis of the position residuals are contained in Tab. 5 for the three receivers.

Table 5: RMS values obtained for SPP and GNSS POWER algorithms in East, North and Up in kinematic scenario. The results are reported for both BRDC and BRDC + SSR processings

	RMS [m]											
	BRDC						BRDC + SSR					
	SPP			GNSS POWER			SPP			GNSS POWER		
	East	North	Up	East	North	Up	East	North	Up	East	North	Up
GEOMAX ZENITH35 PRO	1.25	1.15	2.14	0.95	1.38	2.01	0.83	0.81	1.43	0.87	0.72	0.95
XIAOMI MI 8	3.41	2.27	6.97	2.04	1.30	5.48	2.15	2.09	5.18	1.27	0.96	4.47
GOOGLE PIXEL 4	14.64	18.97	36.65	3.44	1.13	3.15	16.55	18.52	65.59	2.01	1.26	3.34

The results obtained for GNSS POWER algorithm on data from the geodetic receiver demonstrate an improvement for the RMS values of 7.8, 48.2 and 52.6 % in East, North and Up components when SSR corrections are used in combination with broadcast satellite parameters. Focusing on the results including SSR corrections, the comparison between GNSS POWER and SPP algorithm shows a small reduction in R95 values - from 1.62 to 1.60 m - and the RMS values in North and Up. A degradation of 0.04 m in the RMS observed in East direction, this is due to the higher mean values experienced in the residuals (-0.86 with respect to -0.80 m) caused by the initialization of GNSS POWER solution. In the case of the geodetic receiver, such small difference between SPP and GNSS POWER accuracy is probably due to smoothing algorithms automatically enabled within the

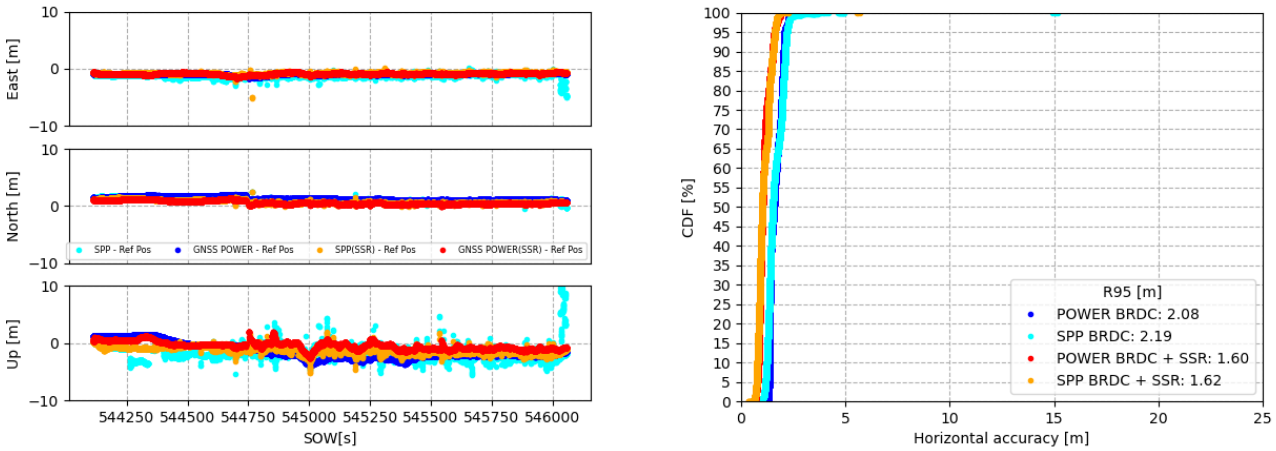

(a) 3D residual position in a local reference frame

(b) CDF for horizontal residuals

Figure 11: Positioning residuals analysis for the geodetical receiver

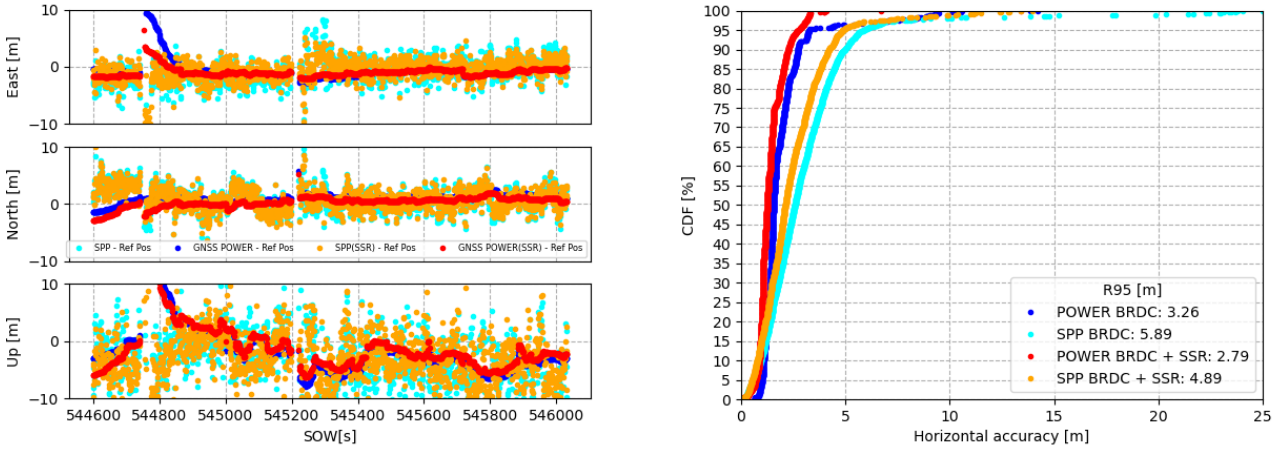

(a) 3D residual position in a local reference frame

(b) CDF for horizontal residuals

Figure 12: Positioning residuals analysis for the Xiaomi Mi 8

GNSS receiver to reduce the pseudorange noise. In fact, the use of GNSS POWER instead of SPP processing strategy on data acquired from the Xiaomi Mi 8 leads to improvements between 40.0 and 50.0 % for the horizontal components and between 13.7 and 21.4 % in vertical direction. Furthermore, the use of SSR corrections allows to obtain RMS of 1.27, 0.96 and 4.47 m in East, North and Up: GNSS POWER solutions are enhanced for the 37.8, 26.4 and 18.4 %. A reduced accuracy with respect to the Xiaomi Mi 8, especially for the SPP approach, is observed with the Google Pixel 4. This is due to outliers not handled within RTKLib as demonstrated in Fig. 13. Neglecting therefore SPP solutions, the use of SSR corrections increases the accuracy in GNSS POWER solutions in East and Up directions: respectively, from 3.44 and 16.55 to 2.01 and 3.34 m. On the other hand, the North direction shows a reduction in the accuracy from 1.13 m to 1.26 m. Nevertheless, the horizontal R95 decreases from 7.97 m to 3.75 m showing the benefits of using SSR corrections in addition to the broadcast satellite information.
The accuracy demonstrated in real-time scenario and stand-alone mode increases the possibility and reliability of lane detection using both geodetic receivers and Android smartphones. Fig. 14 shows the results obtained in a section of the followed track. The geodetic receiver (Fig. 14a) allows to clearly identify the lane in which the car is moving for every lap. Despite the higher noise showed in the results obtained with the Xiaomi Mi 8 (Fig. 14b), the lane is still detectable. Higher uncertainty is observed on the results from Google Pixel 4 reducing the reliability in terms of lane detection.

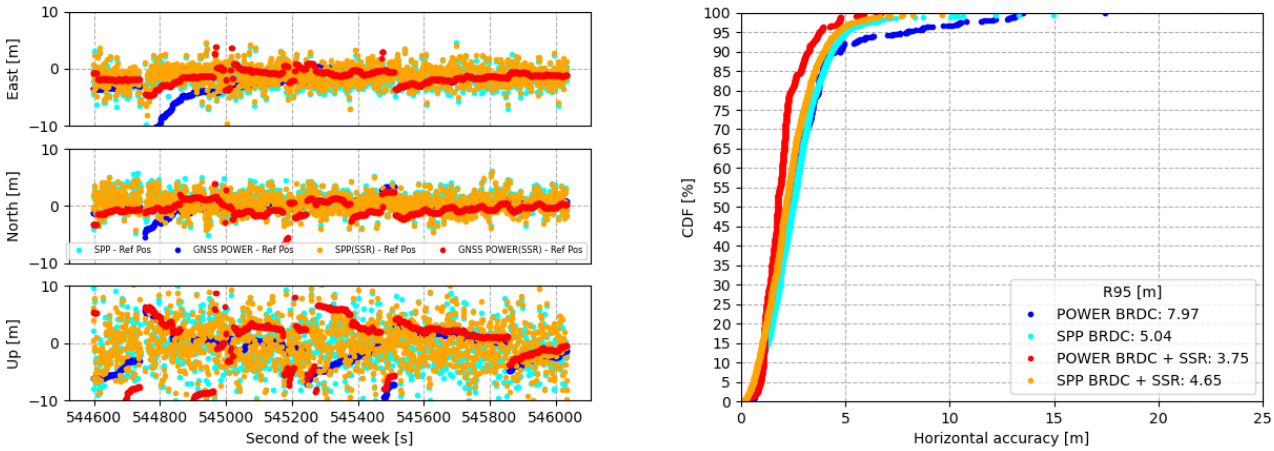

(a) 3D residual position in a local reference frame

(b) CDF for horizontal residuals

Figure 13: Positioning residuals analysis for the Google Pixel 4

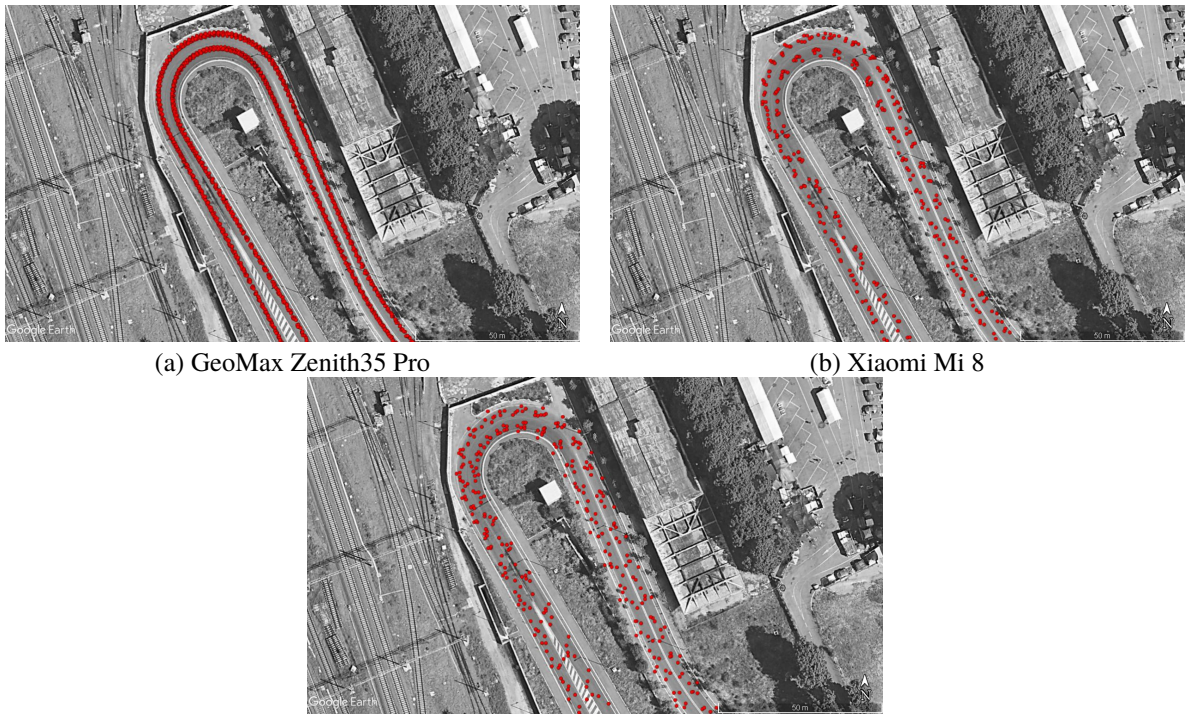

(a) GeoMax Zenith35 Pro

(b) Xiaomi Mi 8

(c) Google Pixel 4

Figure 14: Example of the results obtained in the kinematic scenario

IV. CONCLUSIONS

The effects of SSR orbits, clock and code biases corrections transmitted from the IGS on GNSS POWER PVT solutions was evaluated in this paper. In particular, considering GNSS POWER as the results of a loosley coupling algorithm between position, estimated using SPP, and velocity, estimated using the kin-VADASE, the impact of SSR corrections was also evaluated on these two algorithms.

In particular, the analyses executed in static conditions over one week of 1 Hz GNSS measurements acquired by M0SE, one of the EUREF/IGS reference stations, demonstrated an improvement in the final accuracy achievable with SPP algorithm of 22.7,

17.5 and 29 % in East, North and Up leading to mean RMS, respectively, of 0.31, 0.63 and 1.08 m. When kin-VADASE was tested, on the other hand, the effect of SSR corrections was demonstrated to be negligible when time variation of carrier-phase measurements are analyzed starting from GNSS measurements acquired with high observation rate (>1 Hz). This is due to SSR corrections being constant over very short periods. Moving on GNSS POWER, in this case an improvement of about 32.6, 18.2 and 18.2 % and, therefore, mean RMS of 0.26, 0.60 and 0.99 m in East, North and Up was observed using SSR corrections.

A second test, involving GNSS measurements from a geodetic receiver and two smartphones (one Xiaomi Mi 8 and one Google Pixel 4), was carried out in the scenario of car navigation in urban environment with high sky-visibility. In this case, the use of SSR corrections improved 3D accuracy for all the 3 GNSS receivers. In particular, for the geodetic receiver RMS of 0.87, 0.72 and 0.95 m were obtained in East, North and Up. Considering the same directions, the analysis on the Xiaomi Mi 8 demonstrated accuracy of 1.27, 0.96 and 4.47 m, while the Google Pixel 4 showed RMS of 2.01, 1.26 and 3.34 m. The comparison with RTKLib SPP results demonstrated higher robustness with respect to poor quality GNSS observations especially in the case of Google Pixel 4. The evaluation of horizontal accuracy, through the CDF analysis, demonstrated high reliability in lane-level detection using the geodetic receiver and the Xiaomi Mi 8. R95 of 1.62 and 2.79 m were obtained for the geodetic receiver and Xiaomi Mi 8, respectively. Lower accuracy was obtained using the Google Pixel 4 in this test as demonstrated from the R95 of 3.75 m.

In conclusion, the use of SSR orbits, clock and code biases corrections was proven to be beneficial for SPP and GNSS POWER solutions in order to increase the accuracy in real-time applications. The accuracy level achievable with GNSS POWER, in fact, can support additional kinematic applications, i.e. traffic monitoring, lane level detection and etc., also with mass-market devices, as a Xiaomi Mi 8, in favourable environments.

REFERENCES

[1] P. Bolla and K. Borre, "Performance analysis of dual-frequency receiver using combinations of gps l1, l5, and l2 civil signals," *Journal of Geodesy*, vol. 93, no. 3, pp. 437–447, 2019.

[2] K. Wang, P. Chen, and P. J. Teunissen, "Single-epoch, single-frequency multi-gnss l5 rtk under high-elevation masking," *Sensors*, vol. 19, no. 5, p. 1066, 2019.

[3] B. Eissfeller, C. Tiberius, T. Pany, R. Biberger, and G. Heinrichs, "Real-time kinematic in the light of gps modernization and galileo," in *Proceedings of the 14th International Technical Meeting of the Satellite Division of The Institute of Navigation (ION GPS 2001)*, 2001, pp. 650–682.

[4] J. Zumberge, M. Heflin, D. Jefferson, M. Watkins, and F. Webb, "Precise point positioning for the efficient and robust analysis of gps data from large networks," *Journal of geophysical research: solid earth*, vol. 102, no. B3, pp. 5005–5017, 1997.

[5] G. Wübbena, M. Schmitz, and A. Bagge, "Ppp-rtk: precise point positioning using state-space representation in rtk networks," in *Proceedings of ION GNSS*, vol. 5, 2005, pp. 13–16.

[6] P. Teunissen and A. Khodabandeh, "Review and principles of ppp-rtk methods," *Journal of Geodesy*, vol. 89, no. 3, pp. 217–240, 2015.

[7] A. El-Mowafy, "Performance analysis of the rtk technique in an urban environment," *Australian surveyor*, vol. 45, no. 1, pp. 47–54, 2000.

[8] L. Pan, Z. Xiaohong, and G. Fei, "Ambiguity resolved precise point positioning with gps and beidou," *Journal of Geodesy*, vol. 91, no. 1, pp. 25–40, 2017.

[9] J. Míguez, J. V. Perello-Gisbert, R. Orus-Perez, and J. Garcia-Molina, "Real-time multi-gnss ppp kinematic performance assessment in challenging scenarios," *NAVITEC 2016*, 2016.

[10] M. Fortunato, J. Critchley-Marrows, M. Siutkowska, M. L. Ivanovici, E. Benedetti, and W. Roberts, "Enabling high accuracy dynamic applications in urban environments using ppp and rtk on android multi-frequency and multi-gnss smartphones," in *2019 European Navigation Conference (ENC)*. IEEE, 2019, pp. 1–9.

[11] U. Robustelli, V. Baiocchi, and G. Pugliano, "Assessment of dual frequency gnss observations from a xiaomi mi 8 android smartphone and positioning performance analysis," *Electronics*, vol. 8, no. 1, p. 91, 2019.

[12] M. Branzanti, G. Colosimo, and A. Mazzoni, "Variometric approach for real-time gnss navigation: First demonstration of kin-vadase capabilities," *Advances in Space Research*, vol. 59, no. 11, pp. 2750–2763, 2017.

[13] X. Lin, J. Bergman, F. Gunnarsson, O. Liberg, S. M. Razavi, H. S. Razaghi, H. Rydn, and Y. Sui, "Positioning for the internet of things: A 3gpp perspective," *IEEE Communications Magazine*, vol. 55, no. 12, pp. 179–185, 2017.

[14] X. Zhang, X. Tao, F. Zhu, X. Shi, and F. Wang, "Quality assessment of gnss observations from an android n smartphone and positioning performance analysis using time-differenced filtering approach," *Gps Solutions*, vol. 22, no. 3, p. 70, 2018.

[15] F. Zhu, X. Tao, W. Liu, X. Shi, F. Wang, and X. Zhang, "Walker: Continuous and precise navigation by fusing gnss and mems in smartphone chipsets for pedestrians," *Remote sensing*, vol. 11, no. 2, p. 139, 2019.

[16] W. Liu, X. Shi, F. Zhu, X. Tao, and F. Wang, "Quality analysis of multi-gnss raw observations and a velocity-aided positioning approach based on smartphones," *Advances in Space Research*, vol. 63, no. 8, pp. 2358–2377, 2019.

[17] G. Wübbena, M. Schmitz, and A. Bagge, "Ppp with ambiguity resolution (ar) using rtcm-ssr," in *IGS Workshop (Pasadena, CA, 23–27 June 2014)*, 2014.

[18] M. Kim and K.-D. Park, "Development and positioning accuracy assessment of single-frequency precise point positioning algorithms by combining gps code-pseudorange measurements with real-time ssr corrections," *Sensors*, vol. 17, no. 6, p. 1347, 2017.

[19] G. Colosimo, M. Crespi, and A. Mazzoni, "Real-time gps seismology with a stand-alone receiver: A preliminary feasibility demonstration," *Journal of Geophysical Research: Solid Earth*, vol. 116, no. B11, 2011.

[20] M. Fortunato, M. Ravanelli, and A. Mazzoni, "Real-time geophysical applications with android gnss raw measurements," *Remote Sensing*, vol. 11, no. 18, p. 2113, 2019.

[21] R. S. Committee *et al.*, "Rtcm standard 10403.3 differential gnss (global navigation satellite systems) services-version 3," *RTCM Special Committee*, no. 104, 2016.

[22] Z. Li, J. Zhang, T. Li, X. He, and M. Wu, "Analysis of static and dynamic real-time precise point positioning and precision based on ssr correction," in *2016 IEEE International Conference on Information and Automation (ICIA)*. IEEE, 2016, pp. 2022–2027.

[23] Z. Wang, Z. Li, L. Wang, X. Wang, and H. Yuan, "Assessment of multiple gnss real-time ssr products from different analysis centers," *ISPRS International Journal of Geo-Information*, vol. 7, no. 3, p. 85, 2018.

[24] J. A. Klobuchar, "Ionospheric time-delay algorithm for single-frequency gps users," *IEEE Transactions on aerospace and electronic systems*, no. 3, pp. 325–331, 1987.

[25] T. Takasu and A. Yasuda, "Development of the low-cost rtk-gps receiver with an open source program package rtklib," in *International symposium on GPS/GNSS*. International Convention Center Jeju Korea, 2009, pp. 4–6.

[26] M. Branzanti, G. Colosimo, M. Crespi, and A. Mazzoni, "Gps near-real-time coseismic displacements for the great tohoku-oki earthquake," *IEEE Geoscience and remote sensing letters*, vol. 10, no. 2, pp. 372–376, 2012.

[27] P. Tétreault, J. Kouba, P. Héroux, and P. Legree, "Csrs-ppp: an internet service for gps user access to the canadian spatial reference frame," *Geomatica*, vol. 59, no. 1, pp. 17–28, 2005.